



HAL
open science

Growth behavior and electronic and optical properties of IrGen ($n = 1-20$) clusters

Mustafa Lasmi, Sofiane Mahtout, Franck Rabilloud

► To cite this version:

Mustafa Lasmi, Sofiane Mahtout, Franck Rabilloud. Growth behavior and electronic and optical properties of IrGen ($n = 1-20$) clusters. *Journal of Nanoparticle Research*, 2021, 23 (1), pp.26. 10.1007/s11051-020-05124-x . hal-03167348

HAL Id: hal-03167348

<https://hal.science/hal-03167348>

Submitted on 16 Mar 2021

HAL is a multi-disciplinary open access archive for the deposit and dissemination of scientific research documents, whether they are published or not. The documents may come from teaching and research institutions in France or abroad, or from public or private research centers.

L'archive ouverte pluridisciplinaire **HAL**, est destinée au dépôt et à la diffusion de documents scientifiques de niveau recherche, publiés ou non, émanant des établissements d'enseignement et de recherche français ou étrangers, des laboratoires publics ou privés.

Growth behavior, electronic and optical properties of IrGe_n (n=1-20) clusters

Mustafa Lasmi^a, Sofiane Mahtout^a, Franck Rabilloud^b

*^aLaboratoire de Physique Théorique, Faculté des Sciences Exactes, Université de Bejaia,
06000 Bejaia, Algérie,*

*^bUniv Lyon, Université Claude Bernard Lyon 1, CNRS, Institut Lumière Matière, F-69622,
Villeurbanne, France*

Corresponding authors: mahtout_sofiane@yahoo.fr, franck.rabilloud@univ-lyon1.fr

Abstract

First principles calculations are performed to investigate the structural and electronic properties of small IrGe_n (n = 1–20) clusters. Cage-like configurations where the iridium atom is encapsulated inside a germanium cage are predicted to be favored for n ≥ 12. Doping Ir atom enhances the stability of the corresponding germanium frame. Our results highlight the great stability of IrGe₁₃ which presents a high-symmetry cage like geometry and a peculiar electronic structure in which the valence electrons of Ir and Ge atoms are delocalized and exhibit a shell structure. Absorption spectra, vertical ionization potentials and electron affinities are also calculated and discussed.

1. Introduction

The trend towards miniaturization in electronics, while increasing performance, has triggered interest in small nanoparticles [1]. The properties (electronic, optical, structural, etc.) of nanoparticles and nanoclusters strongly depend on size, shape and chemical composition. In particular, they may change dramatically with the addition or substitution of one or few atoms in the cluster. Accordingly, clusters, used as building blocks, could offer great opportunities to develop self-assembly of nanocrystals and materials with tuned properties [1]. In particular, ultra-stable clusters, e.g. ligand-coated clusters or endohedrally doped cage clusters, are highly desired [2,3].

Germanium is an important semiconductor material widely used in the electronics industry and for nanotechnology applications. At the nanoscale, small and medium-sized germanium clusters have been extensively studied in both theoretical and experimental fields [4-8]. Later, in 2010s, much experimental and theoretical research on Ge_n clusters doped with different transition metal have been reported [3]. The presence of a foreign atom often leads to enhance the stability, as it saturates the dangling bonds, particularly in endohedral structures where the metal atom is encapsulated inside a germanium cage. Also, the metal induces significant changes in electronic and magnetic properties.

Among recent studies on metal-doped clusters, one can cite the works of Deng et al. [9,10] where the structural and magnetic properties of CoGe_n^- and $\text{VGe}_n^{-/0}$ ($n=2-12$) Clusters were investigated using anion photoelectron spectroscopy combined with density functional theory (DFT) calculations. The structural evolution was found to be much related to the electron transfer pattern and the minimization of the magnetic moments for most of these clusters. Several computational studies, mainly at DFT level, have investigated the geometries, stabilities, and electronic properties of NiGe_n ($n = 1-20$) [11-16], WGe_n ($n = 1-17$) [17], ZnGe_n ($n = 1-13$) [18], CrGe_n ($n < 30$) [19-21], CoGe_n ($n = 1-13$) [16,22], FeGe_n ($n \leq 16$) [23,24], Mo_2 -doped Ge_n ($n = 9-15$) [25], MnGe_n ($n = 2-16$) [26], TiGe_n , ZrGe_n , HfGe_n , ($n \leq 21$) [27,28], RuGe_n ($n \leq 12$) [29], VGe_n ($n < 20$) [30], NbGe_n , TaGe_n ($n < 20$) [31], PdGe_n , PtGe_n ($n \leq 20$) [32,33], and noble metal-doped Ge_n clusters [34-38]. A more extensive review can be found in Ref [3, 31]. These studies highlight the dependence of the growth patterns as well as magnetic and electronic properties on the nature of the doping metal. While doping with Cr, Fe, Co, Mn seems to favour high-spin states, the magnetic moment is generally quenched for the other

foreign atom. Most often, the doping atom contributes to strengthen the stability of the germanium framework, and adopts an endohedral position when the number of atoms is enough to form a cage covering the metal atom. This is, e.g., the case for the vanadium atom, for which VGe_{14} shows a relatively high stability in an O_h symmetry cagelike geometry [30]. Similarly, $NbGe_{15}$ and $TaGe_{15}$ adopt a cagelike structure which present a high stability [31]. However, the energetics also depend on the metal, as the early transition metals seem to increase the stability of the germanium framework more strongly than noble metals do.

Iridium presents an unfill atomic 5d shell and is known to be low reactive. Ir-based alloys are widely used in industry. Recently, germanium and iridium based bulk alloys were synthesized and characterized [39,40]. Superconductivity were reported for the compound $TaIr_2Ge_2$, which surprisingly displays a structure based on endohedral $Ta@Ir_7Ge_4$ clusters [39]. Also, small iridium-germanium complexes were synthesized in solution [41].

Here, we investigate the structural and electronic properties of $IrGe_n$ clusters, for which, to the best of our knowledge, no previous study has been reported in the literature. Our purpose in this work is to investigate with an ab initio DFT calculations the effect of one iridium atom on the structural and electronic properties of small germanium cage clusters and their evolution as a function of the size and shape. We hope that our work would be constructive to understand the properties and the growth behavior of $IrGe_n$ clusters and will be guide further theoretical and experimental investigations. This manuscript is organized as follows: the computational details are described in section 2, the structural and energetic properties are presented in section 3 following by a discussion about the electronic and optical properties.

2. Computational Methodology

Geometry optimizations have been performed at the DFT level using the Perdew-Burke-Ernzerhof (PBE) exchange-correlation density functional [42]. The Siesta simulation package was used [43]. A simple cubic cell of side 40 Å has been used for all the clusters to avoid the interaction between the neighboring clusters due to the limit periodic conditions. The geometries were optimized without any symmetry constraints and only the Γ point is used for the Brillouin zone integrations. We have used the norm-conserving Troullier-Martins nonlocal pseudopotentials [44] factorized in the Kleinman-Bylander form [45], together with the double zeta and polarization (DZP) basis set.

At the present level of calculation, the bond length of Ge₂ is found to be 2.450 Å, in agreement with the experimental value of 2.44 Å [46]. That of Ir₂ was calculated at 2.353 Å, compared to the experimental value of 2.35 Å [47]. The binding energy of Ge₂ is 1.44 eV, also in agreement with experimental (~1.35 eV) value [48].

Different spin multiplicity states were systematically tested for all clusters. However, for each cluster the lowest-energy isomers were found to be a doublet. Conjugate gradient algorithm is used for the structures optimizations with the convergence criterion of 10⁻³ eV/Å on the Hellmann-Feynman forces. A complete exploration of geometrical configurations is out of reach. Here, to explore the configuration spaces, a considerable number of possible initial structures (about 10 for very small clusters and about 50 for larger ones) were considered for each size. All isomeric structures obtained by substituting one Ge atom with a metal atom on different sites of the lowest-energy configuration of pure Ge_{n+1} clusters [30] have been considered. We have also tested structures already published for metal-doped Ge_n, and try to build MGe_n by adding one Ge atom to MGe_{n-1}.

The stability of Ge_{n+1} and IrGe_n clusters was obtained by the calculation of the binding energy per atom as defined by the following formula:

$$E_b(\text{Ge}_{n+1}) = ((n+1) E(\text{Ge}) - E(\text{Ge}_{n+1})) / (n + 1) \quad (1)$$

$$E_b(\text{IrGe}_n) = (n E(\text{Ge}) + E(\text{Ir}) - E(\text{IrGe}_n)) / (n + 1) \quad (2)$$

where E(Ge) and E(Ir) are the total energy of free Ge and Ir atoms respectively, and E(Ge_{n+1}) and E(IrGe_n) are the total energy of the corresponding Ge_{n+1} and IrGe_n clusters. The HOMO-LUMO gap is defined as the difference between the Highest Occupied Molecular Orbital and the Lowest Unoccupied Molecular:

$$\Delta E = E(\text{LUMO}) - E(\text{HOMO}) \quad (3)$$

The second-order difference energies of Ge_{n+1} and IrGe_n clusters was calculated by the following expressions:

$$\Delta_2 E(\text{Ge}_{n+1}) = E(\text{Ge}_{n+2}) + E(\text{Ge}_n) - 2 E(\text{Ge}_{n+1}) \quad (4)$$

$$\Delta_2 E(\text{IrGe}_n) = E(\text{IrGe}_{n+1}) + E(\text{IrGe}_{n-1}) - 2 E(\text{IrGe}_n) \quad (5)$$

where E(M) is the total energy of the most stable structure for each cluster M. Finally, we have calculated the vertical ionization potential (VIP) and the vertical electron affinity (VEA):

$$\text{VIP} = E^+ - E \quad (6)$$

$$\text{VEA} = E - E^- \quad (7)$$

where E⁺ is the total energy of the cationic cluster and E⁻ is the total energy of the anionic cluster calculated at the geometry of the corresponding neutral cluster.

Further analysis of the electronic properties and molecular orbitals have been performed with the software Gaussian09 [49] using PBE and the Gaussian-type basis sets cc-pvtz for Ge and LanL2DZ for Ir. They include the electron population analysis, the plot of density of states, as well as the prediction of optical absorption spectra calculated in the framework of the Time-Dependent DFT (TDDFT).

3. Results and discussion

3.1. Structural properties

The most stable structures for IrGe_n are given in Figure 1. Their physical parameters such as the symmetry group, binding energy E_b (eV/atom), HOMO-LUMO gap ΔE (eV), vertical ionization potential VIP (eV) and vertical electron affinity VEA (eV) are given in Table 1. Several low-lying isomers are displayed in Figure S11, while their relative data can be found in Table S1. The global growth pattern of IrGe_n clusters shows that the three-dimensional structures dominate from $n = 4$ and the compact like-spherical structures with Ir atom encapsulated inside a Ge_n cage are observed from size $n = 12$.

The monomer IrGe has a bond length of 2.256 Å and a bonding energy per atom of 1.778 eV. No experimental data is available. IrGe_2 is an isosceles triangle with a binding energy of 2.368 eV, while the lowest-energy structure of IrGe_3 is a rhombus with C_{2v} symmetry and average bond lengths of 2.475 and 2.555 Å for Ge-Ge and Ir-Ge respectively. From $n = 4$, the IrGe_n clusters favor the three dimensional structures. The ground state structure of IrGe_4 is obtained by capping the rhombus structure of IrGe_3 with one extra Ge atom. For IrGe_5 the square bipyramidal geometry with C_s symmetry is found to be the best structure. The geometry of IrGe_6 is a bi-capped pentagonal structure with high C_{5v} symmetry and high binding energy of 3.129 eV. The best isomer of IrGe_7 with C_s symmetry is obtained by capping one GeIrGe triangle of IrGe_6 .

From $n = 8$, the Ir atom adopts an endohedral position and becomes to be highly coordinated, since it makes a bonding with all germanium atoms. Also, from $n=9$, the interatomic bond distances Ir-Ge become larger than those of Ge-Ge (for IrGe_9 , the average Ir-Ge and Ge-Ge bond lengths are 2.728 and 2.699 Å respectively). This constitutes a change in the growth behavior of the IrGe_n clusters. However, for $n = 8-11$, the framework of germanium is an open cage, the cage becomes completely closed at $n=12$. The structures of IrGe_9 , IrGe_{10} and IrGe_{11} are somewhat similar, but added Ge atoms leads to close the germanium backbone.

They have no or low symmetry. The spherical cage-like structure with C_2 symmetry of IrGe_{12} is composed of four pentagonal faces and four diamond faces with a fully encapsulated Ir atom in the center of the structure. A high symmetry C_{4v} structure is obtained as the best isomer of IrGe_{13} . With the binding energy of 3.347 eV, it is the most stable structure of all IrGe_n clusters studied in this work. The Ir atom located at the center of structure is coordinated with all the Ge atoms of the Ge_{12} cage. A structure based on multi rhombus faces with Ir atom at the center and belonging the high symmetry C_{4v} is obtained for the best isomer of IrGe_{14} with a binding energy of 3.322 eV. IrGe_{15} and IrGe_{16} are composed of the IrGe_{14} frame on which one or two Ge atoms are attached. Thus, a capped structure with C_s symmetry is obtained for the best isomer of IrGe_{15} . A distorted cage-like structure with C_1 symmetry is obtained for the best isomers for IrGe_{17} cluster. For IrGe_{18} , the ground state structure is a face-sharing pentagonal pyramid structure with C_s symmetry. In the case of IrGe_{19} , the best isomer is obtained by adding a Ge_2 dimer and a Ge_4 rhombus to the cage-like structure of IrGe_{13} . The structure of IrGe_{20} can be seen as the distorted IrGe_{14} structure on which a rhombus and two isolated atoms are attached.

3.2 Energetics and electronic properties

Figure 2 shows the evolution of the binding energy per atom (formula (1)) with the size n , for IrGe_n and compared to that of Ge_n . The binding energy of IrGe_n clusters gradually increases with n , rapidly for very small clusters up to $n=6$ and then the size dependence become very smooth from $n=7$ to 13. Starting from $n=14$, the binding energy per atom decreases slowly from 3.347 eV for $n=13$ down to 3.254 eV for $n=20$. The curve of the average binding energy presents a local maximum value at $n = 13$ and 15, implying that these clusters are more stable than their neighbors. The binding energies of IrGe_n clusters are always larger than the corresponding pure germanium clusters with the same size. These results indicate that the substitution of Ge by a Ir atom in IrGe_n clusters leads to improve their stabilities which suggesting a higher Ir-Ge bond strength compared with the Ge-Ge bond one. Particularly, a strong improvement of the stability, comparatively to the corresponding pure Ge_{n+1} , is observed from $n>8$. This behavior is due to the absorption of the dangling bonds of the germanium cluster by the doping iridium atoms encapsulated inside of the Ge_n cage.

Another parameter that can reflect the stability of the small clusters is the second-order difference in energy (Δ_2E) defined by the relation (3). It can reflect the relative stabilities of the corresponding clusters. It is generally compared with the relative abundances measured in mass

spectroscopy experiments. The second-order difference of energy for the lowest-energy isomers of IrGe_n clusters are shown in Figure 3. The pronounced positive values of Δ_2E are observed for $n = 3, 6, 13$ and 15 , indicating that these clusters may have special stabilities more favorable than their neighbors.

The chemical stability and activity of the small clusters may be related by the value of the HOMO-LUMO gap, which may reflect the ability for the electron to move from the HOMO to the LUMO orbital. A large HOMO-LUMO gap is related to an enhanced chemical stability. The size dependence of the HOMO-LUMO gap of IrGe_n clusters is shown in figure 4. We observe an oscillating behavior for both Ge_{n+1} and IrGe_n clusters, with a pronounced decreasing tendency for pure Ge_{n+1} with the increasing size of clusters. The gaps of IrGe_n clusters are generally much smaller than those for pure Ge_{n+1} clusters. Local maxima are found for $n = 6, 9, 15$ and 17 , while the very small values observed for $n = 2, 8$ and 12 , reminds a metallic character. Interestingly, all closed cage-like structures, i.e. $n \geq 12$, have a similar HOMO-LUMO gap (about 0.5 eV).

The vertical ionization potential (VIP) and the vertical electron affinity (VEA) of IrGe_n clusters are given in Figures 5 and 6 respectively. The size dependence of VIP shows an oscillating behavior with a global decreasing behavior with increasing size. Remarkable values are found for $n = 3, 6, 13, 15$ and 17 , corresponding to the more pronounced local maxima. The VIP exhibits obvious odd-even oscillations from the size 13 to 20. The size dependence of VEA shows a non-monotone increasing from ~ 0.4 to ~ 3.0 eV. The largest values of VEA are generally observed for large clusters, indicating an increase of the chemical stability. Also, the values of VEA corresponding to $\text{IrGe}_6, \text{IrGe}_{13}$ and IrGe_{15} clusters are larger than their neighbors indicating their special stability. The chemical hardness defined as $\eta = \text{VIP} - \text{VEA}$ can be used to characterize the relative stability of small systems. The size dependence, plotted in Figure 7, shows local maxima for $\text{IrGe}_3, \text{IrGe}_6, \text{IrGe}_{10}, \text{IrGe}_{13}, \text{IrGe}_{15}$ and IrGe_{17} clusters, indicating that these clusters have more stabilities and less reactive than their neighboring. VIP and η of IrGe_n are generally smaller than those of Ge_{n+1} , while VEA of IrGe_n is generally larger.

4. Discussion

Our results highlight a transition from exohedral to endohedral structures occurring at $n = 8-12$. From $n=8$, Ir is located at an endohedral site, but the encapsulating cage of germanium is fully closed at $n = 12$. This structural modification strongly affects the electronic properties. The atomic charge and the electron configuration on the metal atom have been estimated

through a natural population analysis [50] (Table 2). For smaller cluster, Ir is located on exohedral site, and its atomic charge is relatively low (between -0.5 and -1 |e|). But, starting from $n = 8$, the charge strongly increases to about -2.5 a.u. The transition at $n = 8$ appears clearly, as q_{Ir} increases from -1.06 to -2.10|e| for $n = 7$ and 8 respectively. Each additional bonding with Ge leads to an increase of the electronic charge on Ir. In the doublet state, the electron configuration of the isolated atom Ir is $6s^1 5d^8$. The additional electrons captured by the metal atom are mainly associated to 5d and 6p electron configurations. In cage-like structure, the gain on 6p becomes dominant. The large atomic charges indicate that the metal interacts with several Ge atoms, thus playing a stabilizing role of the Ge_n cage.

Among all $IrGe_n$ clusters, $IrGe_{13}$ presents a relatively high stability. It has the larger binding energy (Figure 2), a relatively high second-order energy difference (Figure 3), and relatively high values for VIP, EAV, and chemical hardness (Figures 5-7). Beside its atomic structure belongs the C_{4v} symmetry group. In Figure 8, we give the density of states (DOS) together with the Kohn-Sham orbitals calculated at PBE/cc-pvtz(Ge)/LanL2DZ(Ir) level. Electronic shells can easily be identified, with their S, P, D, F, and G character. Actually, the reorganization of the valence electrons from Ge and Ir atoms, i.e. $3s_{Ge}$, $3p_{Ge}$ and $5d_{Ir}$, $6s_{Ir}$ electrons, leads to a shell structure where orbitals are delocalized on the whole cluster. Hence, the 61 electrons fill the sequence $1S^2 1P^6 1D^{10} 1F^{14} 2S^2 2D^{10} 2P^6 1G^{11}$. Such a pooling of electrons has been already found for VGe_{14} [30], $CuGe_{10}$ [37], $PdGe_{16}$ [32].

To further characterize the clusters, we present in Figure 9 (and Figure S2) the absorption spectra of $IrGe_n$. For the molecule $IrGe$, the first optical transition is found at 3.6 eV, it corresponds to the excitation from d_{Ir} to $s_{Ir} + p_{Ge}$ orbitals. Then, there is a transition at 4.75 eV with a very low oscillator strength, and the absorption becomes intense from 5.7 eV. Most of excitations between 5 and 10 eV correspond to transitions from d_{Ir} to $s_{Ir} + p_{Ge}$ orbitals as well. To our knowledge, no experimental and theoretical data is available. For all clusters, a strong response is found in the UV range of energy. When the number of Ge atoms and the number of Ir-Ge bonds increase, the density of states become much higher. Thus, the absorption spectra of endohedral structures show an increasing response in the UV. For $IrGe_{13}$, a first optical excitation is calculated at 3.55 eV, which corresponds to the transitions from the shells 2P and 2D to the unfilled 1G shell. Between 4 and 5 eV, several excitations from the super shell 1G to 1H are observed. In a very recent work, we have showed that the absorption spectra of $PdGe_n$ and $PtGe_n$ are few dependent on the position of the metal atom (exo versus endohedral position), while the density of states is much higher in the case of surface-bound metal due to a lower symmetry of the structure. The low dependency of the absorption spectra on the geometrical

structure can be explained by the electronic arrangement which tends to favor the pooling of valence electrons and the organization in shells where electrons occupy orbitals fully delocalized over the whole volume of the cluster. The pooling of electrons is likely to be somewhat independent of the details of the structure, and consequently the optical absorption as well.

5. Conclusions

We have performed a systematic investigation of the geometry and the electronic properties of the iridium-doped germanium clusters by using DFT calculations. The growth pattern shows that the iridium atom occupies a peripheral position for very small clusters ($n < 8$). For $n \geq 8$, Ir moves to the endohedral position and becomes highly coordinated. From $n = 12$, it is completely encapsulated by the germanium cage. The substitution of one Ge atom by one Ir atom enhances considerably the stability of the host cluster. The calculated binding energy, the second-order energy difference, the HOMO–LUMO gaps and vertical ionization potential and electron affinities manifest the large stability of the $\text{IrGe}_{6,13,15}$ clusters. The HOMO-LUMO gap calculations show that the chemical activity of IrGe_n clusters is generally higher than that of the corresponding pure Ge_{n+1} clusters. The optical absorption spectra highlight a strong response in the UV domain.

Acknowledgements

This work was supported by the open research fund of the “General Direction of Research and Technological Development DGRSDT” of the “Ministry of Higher Education and Scientific Research”, Algeria. FR thanks the GENCI-IDRIS (Grant A0070807662) center for generous allocation of computational time.

Declaration of Competing Interest

The authors declare that they have no known competing financial interests or personal relationships that could have appeared to influence the work reported in this paper.

Supplementary material

Table S1. Symmetry group, binding energy E_b (eV/atom), HOMO-LUMO gap ΔE (eV), vertical ionization potential VIP (eV), vertical electron affinity VEA (eV), chemical hardness η (eV) for some lower-energy isomers of IrGe_n clusters.

Figure S1. Lowest-energy structures and their corresponding isomers of IrGe_n clusters ($n=1-20$). For each size, the most stable structure is indicated in bold. Relative energies are given in eV/atom.

Figure S2. Absorption spectra of IrGe_n ($n=1-20$). The calculated absorption spectra shown in the figure give the oscillator strength as a function of the excitation energy together with a curve obtained by a Lorentz broadening with a full width at half-maximum (fwhm) of 0.08 eV.

Table 1. Symmetry group, binding energy E_b (eV/atom), HOMO-LUMO gap ΔE (eV), vertical ionization potential VIP (eV), vertical electron affinity VEA (eV), chemical hardness η (eV) and average bond length a_{Ge-Ge} (Å) and a_{Ir-Ge} (Å) for the most stable isomers of $IrGe_n$ clusters.

Cluster	Symmetry group	E_b (eV/atom)	ΔE (eV)	VIP (eV)	VEA (eV)	a_{Ge-Ge} (Å)	a_{Ir-Ge} (Å)
IrGe	C_∞	1.778	0.705	6.546	0.441	-	2.256
IrGe₂	C_{2v}	2.368	0.302	6.903	1.357	2.617	2.410
IrGe₃	C_{2v}	2.755	0.506	7.196	1.600	2.475	2.555
IrGe₄	C_s	2.879	0.452	6.938	1.707	2.682	2.655
IrGe₅	C_s	3.002	0.254	7.051	2.244	2.742	2.577
IrGe₆	C_{5v}	3.129	0.875	7.075	2.341	2.708	2.662
IrGe₇	C_s	3.136	0.572	6.600	2.197	2.741	2.739
IrGe₈	C_s	3.177	0.284	6.784	2.708	2.748	2.663
IrGe₉	C_2	3.221	0.960	6.368	2.427	2.699	2.728
IrGe₁₀	C_1	3.248	0.860	6.648	2.605	2.708	2.809
IrGe₁₁	C_1	3.307	0.762	6.619	2.777	2.746	2.796
IrGe₁₂	C_2	3.329	0.349	6.626	3.001	2.619	2.830
IrGe₁₃	C_{4v}	3.347	0.443	6.808	3.066	2.602	2.865
IrGe₁₄	C_{4v}	3.322	0.495	5.798	2.279	2.669	2.872
IrGe₁₅	C_s	3.328	0.580	6.494	2.961	2.692	2.960
IrGe₁₆	C_2	3.305	0.472	5.901	2.531	2.767	2.939
IrGe₁₇	C_1	3.277	0.677	6.519	2.944	2.662	2.869
IrGe₁₈	C_s	3.269	0.499	6.021	2.809	2.696	2.933
IrGe₁₉	C_s	3.271	0.592	6.151	2.900	2.747	2.904
IrGe₂₀	C_1	3.254	0.573	5.990	2.853	2.825	2.939

Table 2. Atomic charge q_{Ir} (in a.u., |e|) and electron configuration on Ir atom from the natural population analysis.

Cluster	q_{Ir}	Electron configuration on Ir
IrGe	-0.53	$6s^{1.46} 5d^{8.05} 6p^{0.04}$
IrGe ₂	-0.72	$6s^{1.06} 5d^{8.54} 6p^{0.12} 7s^{0.01}$
IrGe ₃	-0.66	$6s^{0.84} 5d^{8.54} 6p^{0.29} 7p^{0.01}$
IrGe ₄	-0.61	$6s^{0.71} 5d^{8.64} 6p^{0.25} 7p^{0.01}$
IrGe ₅	-0.81	$6s^{0.78} 5d^{8.63} 6p^{0.41} 7p^{0.01}$
IrGe ₆	-0.88	$6s^{0.74} 5d^{8.62} 6p^{0.52} 7p^{0.02}$
IrGe ₇	-1.06	$6s^{0.75} 5d^{8.68} 6p^{0.63} 7p^{0.01}$
IrGe ₈	-2.10	$6s^{0.72} 5d^{8.91} 6p^{1.47} 6d^{0.01}$
IrGe ₉	-2.44	$6s^{0.61} 5d^{9.04} 6p^{1.89} 7s^{0.01} 6d^{0.01}$
IrGe ₁₀	-2.11	$6s^{0.62} 5d^{8.91} 6p^{1.58} 6d^{0.01}$
IrGe ₁₁	-2.54	$6s^{0.61} 5d^{9.04} 6p^{1.89} 7s^{0.01} 6d^{0.01}$
IrGe ₁₂	-2.59	$6s^{0.57} 5d^{9.03} 6p^{1.98} 7s^{0.01} 6d^{0.01}$
IrGe ₁₃	-2.36	$6s^{0.58} 5d^{8.97} 6p^{1.80} 7s^{0.01} 6d^{0.01}$
IrGe ₁₄	-2.59	$6s^{0.57} 5d^{9.11} 6p^{1.91} 7s^{0.01}$
IrGe ₁₅	-2.18	$6s^{0.58} 5d^{9.01} 6p^{1.59} 7s^{0.01}$
IrGe ₁₆	-2.33	$6s^{0.57} 5d^{9.10} 6p^{1.66} 7s^{0.01}$
IrGe ₁₇	-2.26	$6s^{0.57} 5d^{9.03} 6p^{1.66} 6d^{0.01}$
IrGe ₁₈	-2.07	$6s^{0.57} 5d^{9.02} 6p^{1.48} 7p^{0.01}$
IrGe ₁₉	-2.33	$6s^{0.57} 5d^{9.13} 6p^{1.64}$
IrGe ₂₀	-2.12	$6s^{0.57} 5d^{9.05} 6p^{1.51} 7p^{0.01}$

Figure captions

Figure 1. Most stable structures for IrGe_n clusters (n=1-20) together with their spatial symmetry group.

Figure 2. Binding energy (eV/atom) of the lowest-energy structures of Ge_{n+1} [30] and IrGe_n (n=1-20) clusters.

Figure 3. Second-order energy difference (eV) of the lowest-energy structures of Ge_{n+1} [30] and IrGe_n (n=1-20) clusters.

Figure 4. HOMO-LUMO gap (eV) of the lowest-energy structures of Ge_{n+1} [30] and IrGe_n (n=1-20) clusters.

Figure 5. Vertical ionization potential VIP (eV) of the lowest-energy structures of Ge_{n+1} [30] and IrGe_n (n=1-20) clusters.

Figure 6. Vertical electron affinity VEA (eV) of the lowest-energy structures of Ge_{n+1} [30] and IrGe_n (n=1-20) clusters.

Figure 7. Chemical hardness η (eV) of the lowest-energy structures of Ge_{n+1} [30] and IrGe_n (n=1-20) clusters.

Figure 8. Density of states (DOS) of IrGe₁₃ for alpha spin electrons. For each band, the Kohn-Sham orbitals are plotted. Plotted with the software Gabedit[51].

Figure 9. Absorption spectra of IrGe_n(n=1-15). More detailed spectra are available in Figure S2 for IrGe_n (n=1-20).

References

- [1] F. Calvo (ed) (2020) Nanoalloys: from fundamentals to emergent applications, 2nd edition, Elsevier. ISBN: 9780128223888
- [2] K.D. Sattler (ed) (2017) Handbook of nanophysics clusters and fullerenes. CRC, Boca Raton. ISBN: 978-0-12-819847-6.
- [3] Zhao J, Du Q, Zhou S, Kumar V (2020) Endohedrally doped cage clusters. Chem. Rev. 120:9021-9163.
- [4] Bals S, Van Aert S, Romero C P, Lauwaet K, Van Bael M J, Schoeters B, Partoens B, Yücelen E, Lievens P, Van Tendeloo G (2012) Atomic scale dynamics of ultrasmall germanium clusters. Nature Communications 3:897.
- [5] Li B-X, Liang F S, Zhu Y, Xu J, Lai G (2005) Stable structures of neutral and ionic Ge_n (n=11–19) clusters. Journal of Molecular Structure: THEOCHEM 756:19–24.
- [6] Ma S, Wang G (2006) Structures of medium size germanium clusters. Journal of Molecular Structure: THEOCHEM 767:75–79.
- [7] Wang L, Zhao J (2008) Competition between supercluster and stuffed cage structures in medium-sized Ge_n (n=30–39) clusters. The Journal of Chemical Physics 128:024302.
- [8] Zhao L-Z, Lu W-C, Qin W, Zang Q-J, Wang C-Z, Ho K-M (2008) Fragmentation behavior of Ge_n clusters (2<n<33). Chemical Physics Letters 455:225–231.
- [9] Deng X-J, Kong X-Y, Xu X L, Xu H-G, Zheng W-J (2014) Structural and magnetic properties of CoGe_n⁻ (n =2-11) clusters: photoelectron spectroscopy and density functional calculations. ChemPhysChem 15:3987–3993.
- [10] Deng X-J, Kong X-Y, Xu H-G, Xu X-L, Feng G, Zheng W-J (2015) Photoelectron spectroscopy and density functional calculations of VGe_n⁻ (n = 3–12) clusters. The Journal of Physical Chemistry C 119:11048–11055.
- [11] Lu J, Nagase S (2003) Metal-doped germanium clusters MGe_n at the sizes of n=12 and 10: divergence of growth patterns from the MSi_n clusters. Chemical Physics Letters 372:394–398.
- [12] Wang J, Han J-G (2006) A Theoretical study on growth patterns of Ni-doped germanium clusters. The Journal of Physical Chemistry B 110:7820–7827.
- [13] King R-B, Silaghi-Dumitrescu I, Uță M M (2009) Endohedral nickel, palladium, and platinum atoms in 10-Vertex germanium clusters: competition between bicapped square

antiprismatic and pentagonal prismatic structures. *The Journal of Physical Chemistry A* 113:527–533.

[14] Bandyopadhyay D, Sen P (2010) Density functional investigation of structure and stability of Ge_n and Ge_nNi ($n = 1-20$) clusters: validity of the electron counting rule. *The Journal of Physical Chemistry A* 114:1835–1842.

[15] Tang C, Liu M, Zhu W, Deng K (2011) Probing the geometric, optical, and magnetic properties of 3d transition-metal endohedral Ge_{12}M ($\text{M}=\text{Sc}-\text{Ni}$) clusters. *Computational and Theoretical Chemistry* 969:56–60.

[16] Kapila N, Jindal V K, Sharma H (2011) Structural, electronic and magnetic properties of Mn, Co, Ni in Ge_n for ($N=1-13$). *Physica B: Condensed Matter* 406:4612–4619.

[17] Wang J, Han J-G (2006) Geometries and electronic properties of the tungsten-doped germanium clusters: WGe_n ($n = 1-17$). *The Journal of Physical Chemistry A* 110:12670–12677.

[18] Wang J, Han J-G (2007) The growth behaviors of the Zn-doped different sized germanium clusters: a density functional investigation. *Chemical Physics* 342:253–259.

[19] Hou X-J, Gopakumar G, Lievens P, Nguyen M T (2007) Chromium-doped germanium clusters CrGe_n ($n = 1-5$): geometry, electronic structure, and topology of chemical bonding. *The Journal of Physical Chemistry A* 111:13544–13553.

[20] Kapila N, Garg I, Jindal V K, Sharma H (2012) First principles investigation into structural growth and magnetic properties in Ge_nCr clusters for $n=1-13$. *Journal of Magnetism and Magnetic Materials* 324:2885–2893.

[21] Mahtout S, Tariket Y (2016) Electronic and magnetic properties of CrGe_n ($15 \leq n \leq 29$) clusters: a DFT study. *Chemical Physics* 472:270–277.

[22] Jing Q, Tian F, Wang Y (2008) No quenching of magnetic moment for the Ge_nCo ($n=1-13$) clusters: first-principles calculations. *The Journal of Chemical Physics* 128:124319.

[23] Zhao W-J, Wang Y-X (2008) Geometries, stabilities, and electronic properties of FeGe_n ($n=9-16$) clusters: density-functional theory investigations. *Chemical Physics* 352:291–296.

[24] Sosa-Hernández E M, Alvarado-Leyva P G (2009) Magnetic properties of stable structures of small binary clusters. *Physica E: Low-dimensional Systems and Nanostructures* 42:17–21.

[25] Wang J, Han J-G (2008) Geometries, stabilities, and vibrational properties of bimetallic Mo_2 -doped Ge_n ($n = 9-15$) clusters: a density functional investigation. *The Journal of Physical Chemistry A* 112:3224–3230.

- [26] Zhao W-J, Wang Y-X (2009) Geometries, stabilities, and magnetic properties of MnGe_n ($n=2-16$) clusters: density-functional theory investigations. *Journal of Molecular Structure: THEOCHEM* 901:18–23.
- [27] Kumar M, Bhattacharyya N, Bandyopadhyay D (2012) Architecture, Electronic structure and stability of TM@Ge_n (TM = Ti, Zr and Hf; $n = 1-20$) clusters: a density functional modelling. *Journal of Molecular Modeling* 18:405–418.
- [28] Jaiswal S, Kumar V (2016) Growth behavior and electronic structure of neutral and anion ZrGe_n ($n = 1-21$) clusters. *Computational and Theoretical Chemistry* 1075:87–97.
- [29] Jin Y, Tian Y, Kuang X, Lu X, Cabellos J L, Mondal S, Merino G (2016) Structural and electronic properties of ruthenium-doped germanium clusters. *The Journal of Physical Chemistry C* 120:8399–8404.
- [30] Siouani C, Mahtout S, Safer S, Rabilloud F (2017) Structure, stability, and electronic and magnetic properties of VGe_n ($n = 1-19$) clusters. *The Journal of Physical Chemistry A* 121:3540–3554.
- [31] Siouani C, Mahtout S, Rabilloud F (2019) Structure, stability, and electronic properties of niobium-germanium and tantalum-germanium clusters. *Journal of Molecular Modeling* 25:113.
- [32] Lasmi M, Mahtout S, Rabilloud F (2020) The effect of palladium and platinum doping on the structure, stability and optical properties of germanium clusters: DFT study of PdGe_n and PtGe_n ($n=1-20$) clusters. *Computational and Theoretical Chemistry* 1181:112830.
- [33] Trivedi R, Mishra V (2020) Exploring the structural stability order and electronic properties of transition metal M@Ge_{12} (M = Co, Pd, Tc, and Zr) doped germanium cage clusters - A density functional simulation. *J. Mol. Struct.*
<https://doi.org/10.1016/j.molstruc.2020.129371>
- [34] Wang J, Han J-G (2005) A computational investigation of copper-doped germanium and germanium clusters by the density-functional theory. *The Journal of Chemical Physics* 123:244303.
- [35] Bandyopadhyay D (2012) Architectures, electronic structures, and stabilities of Cu-doped Ge_n clusters: density functional modelling. *Journal of Molecular Modeling* 18:3887–3902.
- [36] Li X, Su K, Yang X, Song L, Yang L (2013) Size-selective effects in the geometry and electronic property of bimetallic Au–Ge nanoclusters. *Computational and Theoretical Chemistry* 1010:32–37.

- [37] Mahtout S, Siouani C, Rabilloud F (2018) Growth behavior and electronic structure of noble metal-doped germanium clusters. *The Journal of Physical Chemistry A* 122:662–677.
- [38] Bandyopadhyay D (2019) Electronic structure and stability of anionic AuGe_n (n = 1–20) clusters and assemblies: a density functional modelling. *Struct. Chem.* 30:955-963.
- [39] Srivichitranond L C, Seibel E M, Xie W, Sobczak Z, Klimczuk T, Cav R J (2017) Superconductivity in a new intermetallic structure type based on endohedral Ta@Ir₇Ge₄ clusters. *Phys. Rev. B* 95:174521.
- [40] Szlawska M, Griбанov A, Griбанova S, Kaczorowski D (2018) Ferromagnetic Kondo lattice Ce₂IrGe₃. *Intermetallics* 93:106-112.
- [41] Adams R D, Trufan E (2010) Iridium-germanium and -tin carbonyl complexes. *Organometallics*, 29:4346-4353.
- [42] Perdew J P, Burke K, Ernzerhof M (1997) Generalized gradient approximation made simple. *Phys. Rev. Lett.* 78:1396.
- [43] Soler J M, Artacho E, Gale J D, García A, Junquera J, Ordejón P, Sánchez-Portal D (2002) The SIESTA method for ab initio order-N materials simulation. *J. Phys.: Cond. Matter* 14:2745–2779.
- [44] Troullier N, Martins J L (1991) Efficient pseudopotentials for plane-wave calculations. *Phys. Rev. B: Condens. Matter Mater. Phys.* 43:1993–2006.
- [45] Kleinman L, Bylander D M (1982) Efficacious form for model pseudopotentials. *Phys. Rev. Lett.* 48:1425–1428.
- [46] Gadiyak G V, Morokov Y N, Mukhachev A G, Chernov S V (1982) Electron density functional method for molecular system calculations. *J. Struct. Chem.* 22:670–674.
- [47] Jules J L, Lombardi J R (2003) Transition metal dimer internuclear distances from measured force constants. *J. Phys. Chem. A* 107:1268-1273.
- [48] Kingcade J E, Nagarathna-Naik H M, Shim I, Gingerich K A (1986) Electronic structure and bonding of the molecule from all-electron ab initio calculations and equilibrium measurements. *J. Phys. Chem.* 90:2830-2834.
- [49] Frisch M J et al. (2013), Gaussian09, Revision D.01, Gaussian Inc., Wallingford CT.
- [50] Reed A E, Weinhold F (1983) Natural bond orbital analysis of near-Hartree–Fock water dimer. *J. Chem. Phys.* 78:4066.
- [51]. Allouche A R (2011) A Graphical user interface for computational chemistry software. *J. Comput. Chem.* 32:174-182.

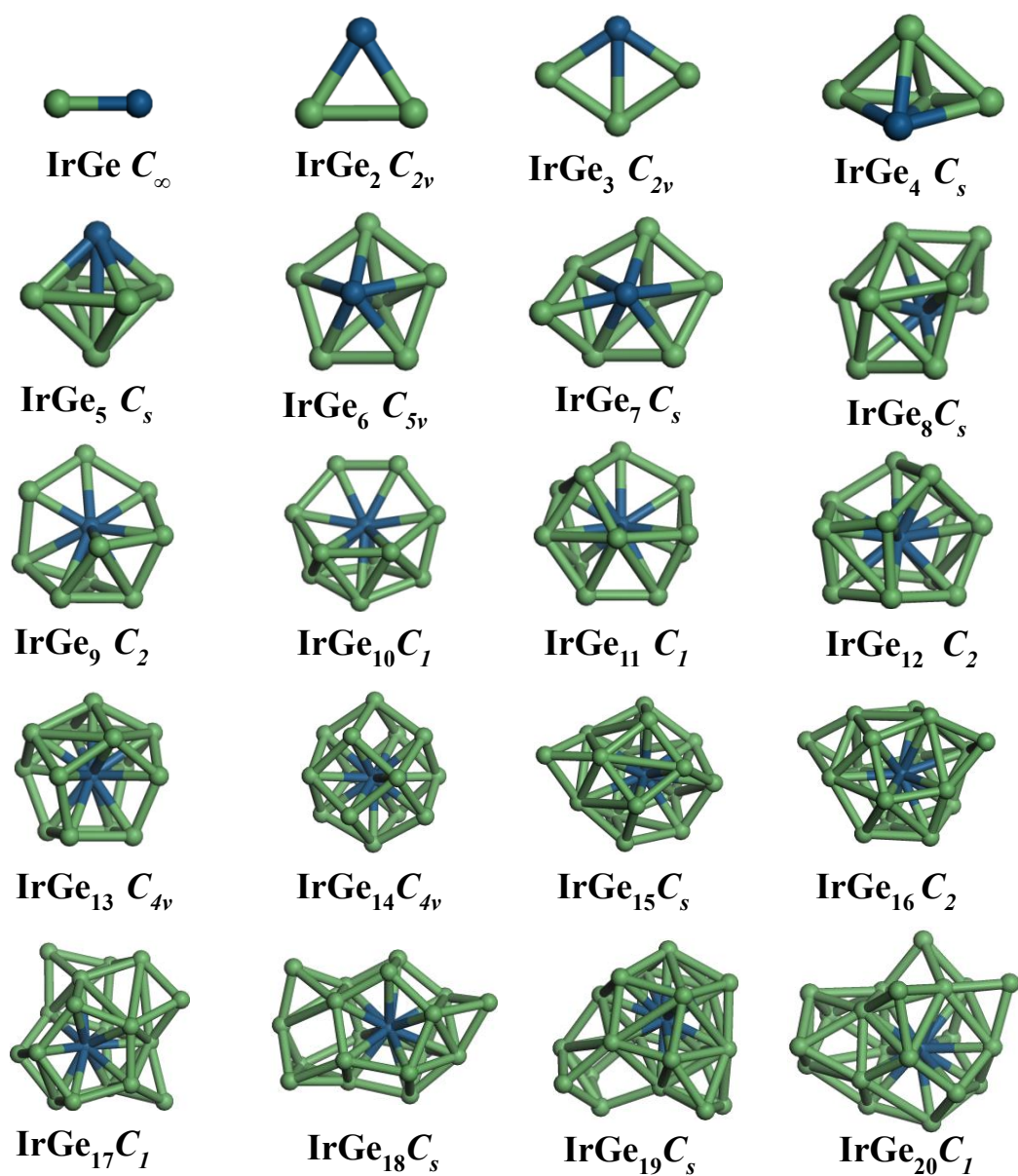


Figure 1. Most stable structures for IrGe_n clusters (n=1-20) together with their spatial symmetry group.

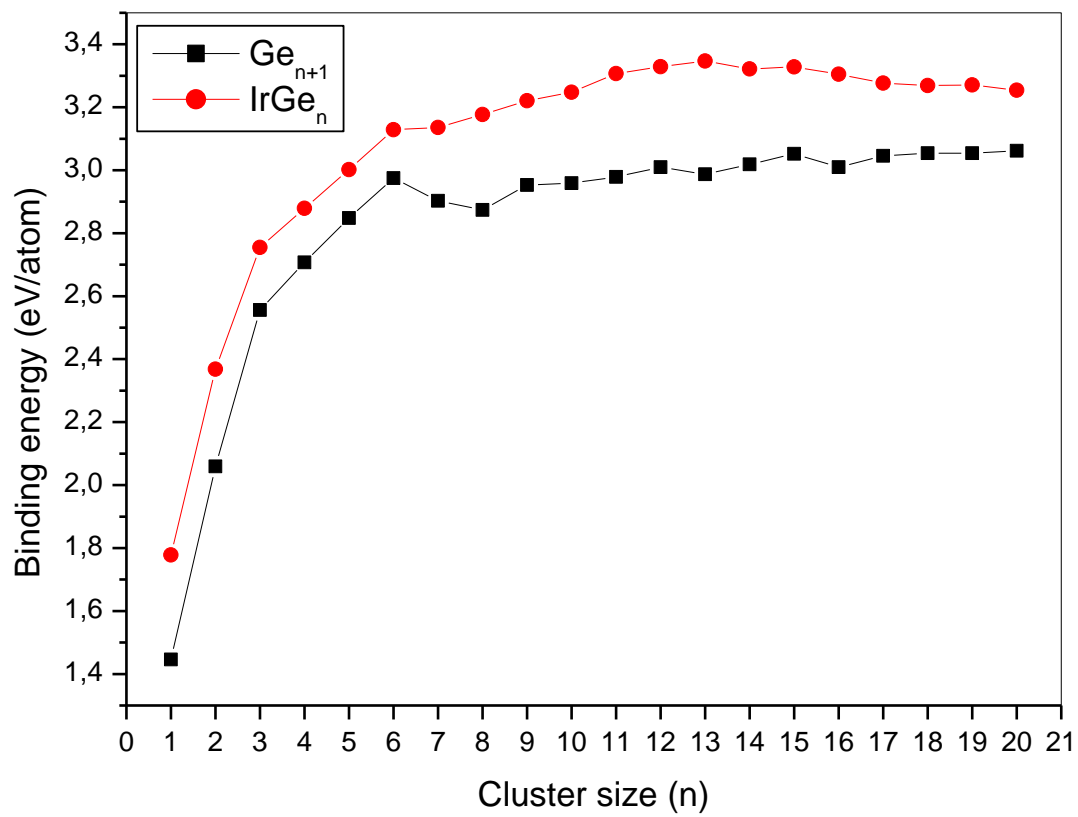


Figure 2. Binding energy (eV/atom) of the lowest-energy structures of Ge_{n+1} [30] and IrGe_n ($n=1-20$) clusters.

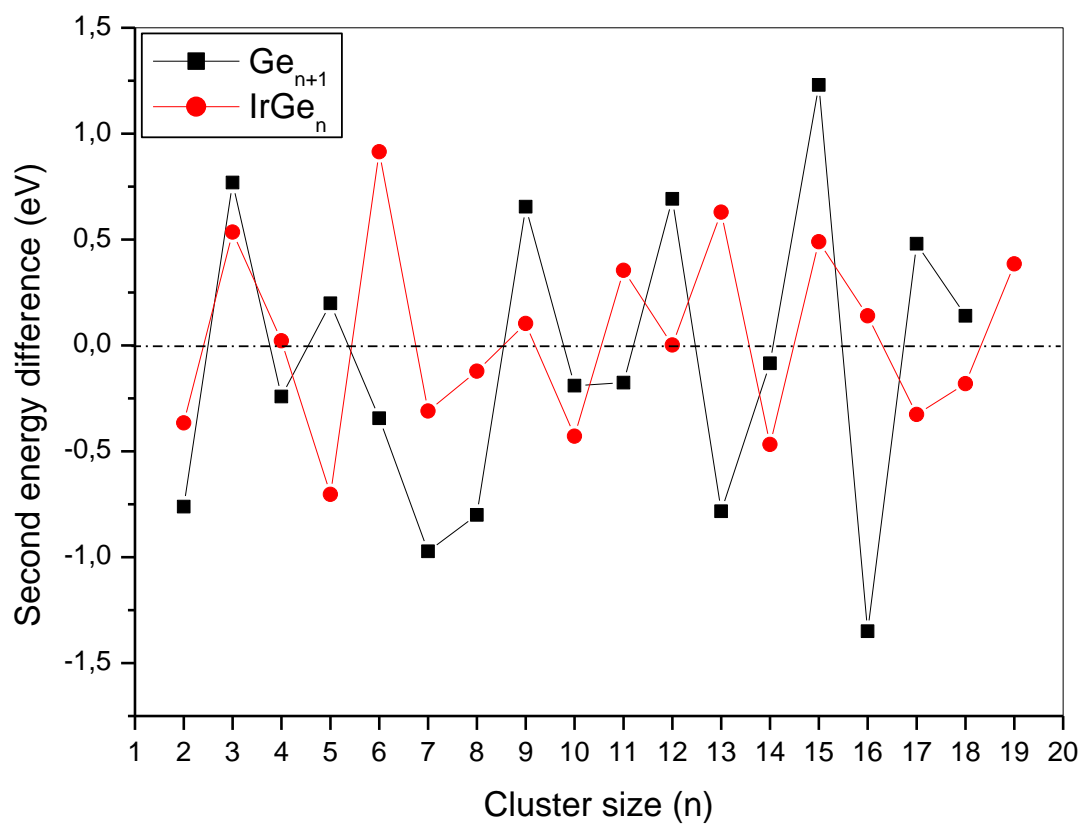


Figure 3. Second-order energy difference (eV) of the lowest-energy structures of Ge_{n+1} [30] and $IrGe_n$ ($n=1-20$) clusters.

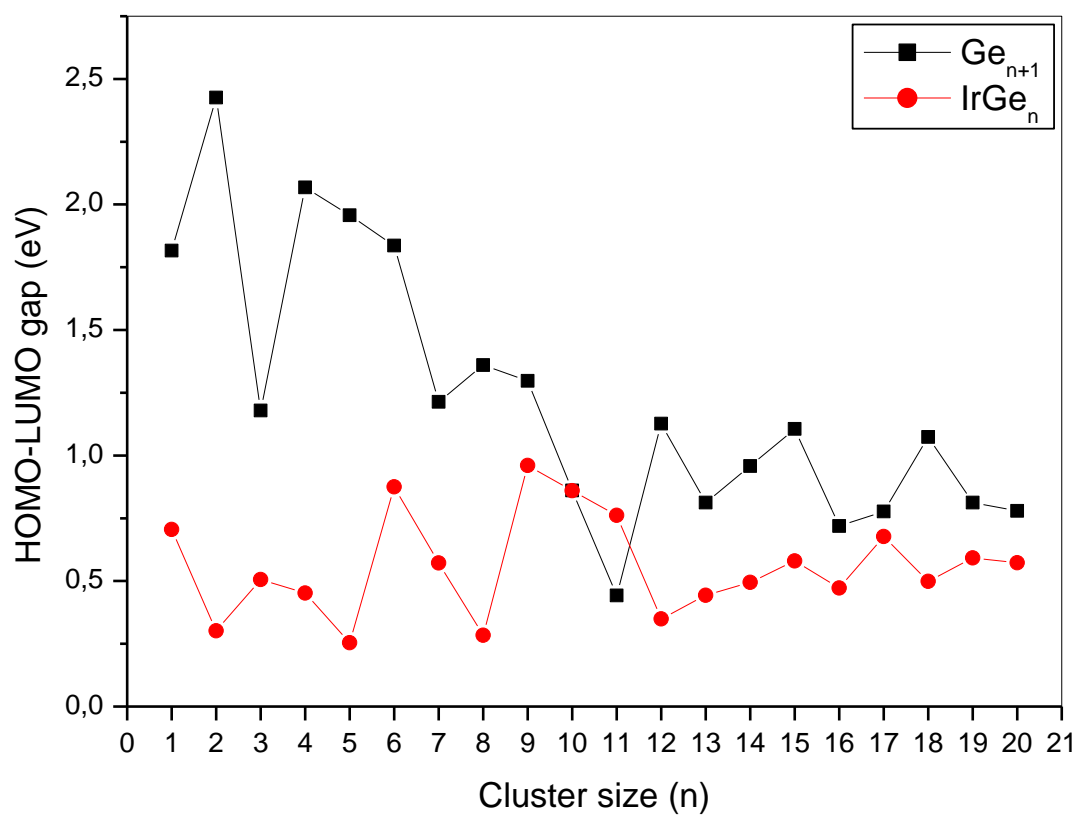


Figure 4. HOMO-LUMO gap (eV) of the lowest-energy structures of Ge_{n+1}[30] and IrGe_n (n=1-20) clusters.

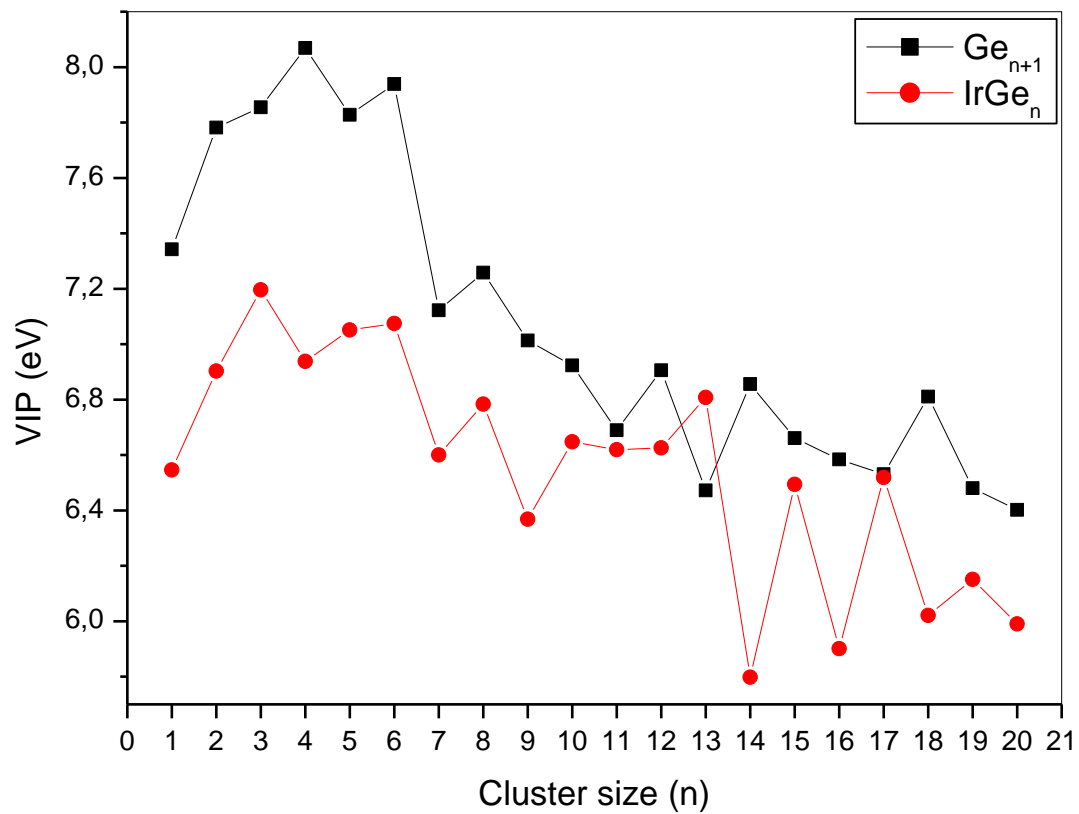


Figure 5. Vertical ionization potential VIP (eV) of the lowest-energy structures of Ge_{n+1} [30] and IrGe_n (n=1-20) clusters.

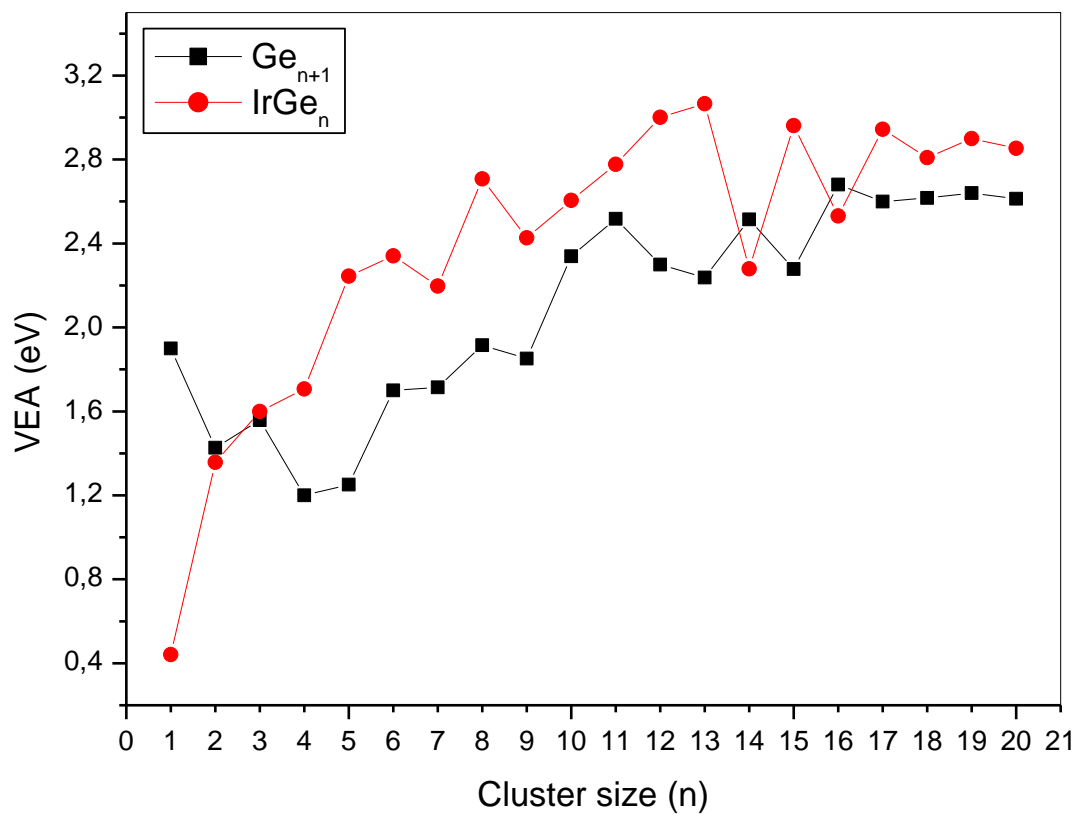


Figure 6. Vertical electron affinity VEA (eV) of the lowest-energy structures of Ge_{n+1} [30] and IrGe_n (n=1-20) clusters.

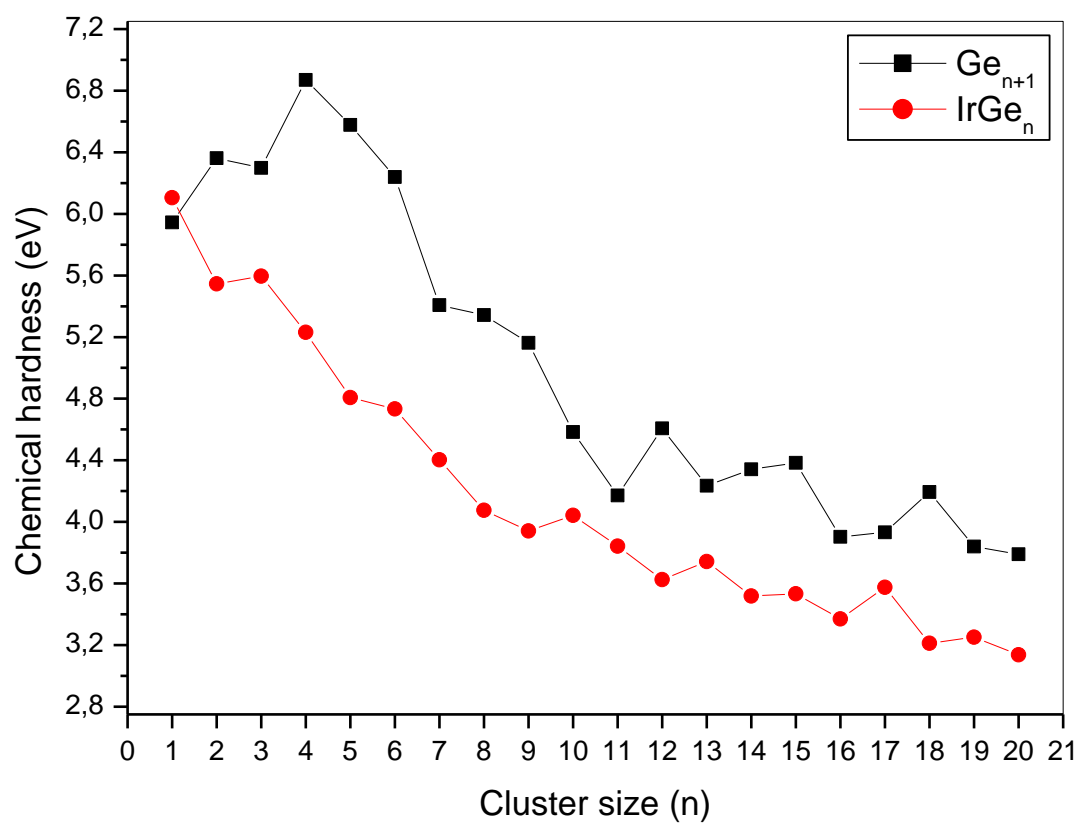


Figure 7. Chemical hardness η (eV) of the lowest-energy structures of Ge_{n+1} [30] and IrGe_n ($n=1-20$) clusters.

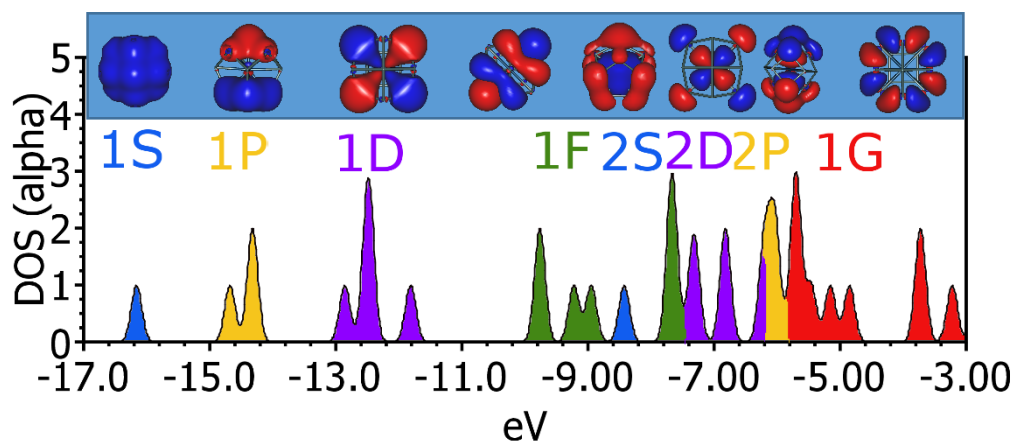


Figure 8. Density of states (DOS) of IrGe13 for alpha spin electrons. For each band, the Kohn-Sham orbitals are plotted. Plotted with the software Gabedit[51].

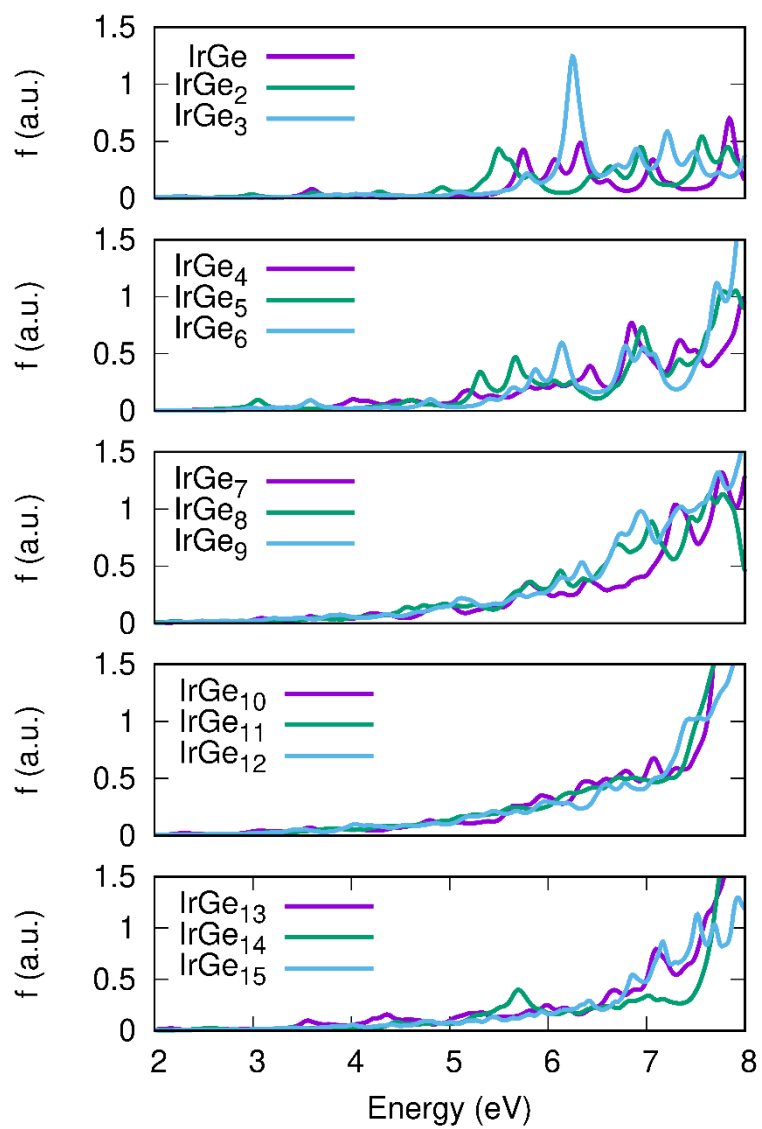


Figure 9. Absorption spectra of IrGe_n ($n=1-15$). More detailed spectra are available in Figure S2 for IrGe_n ($n=1-20$).